

Lensing rates of gravitational wave signals displaying beat patterns detectable by (B-)DECIGO

Shaoqi Hou

School of Physics and Technology, Wuhan University, Wuhan, Hubei 430072, China

Hai Yu

*Department of Astronomy, School of Physics and Astronomy,
Shanghai Jiao Tong University, Shanghai, 200240, China*

Marek Biesiada

*Department of Astronomy, Beijing Normal University, Beijing 100875, China and
National Centre for Nuclear Research, Pasteura 7, 02-093 Warsaw, Poland*

Xi-Long Fan

School of Physics and Technology, Wuhan University, Wuhan, Hubei 430072, China

Seiji Kawamura

Department of Physics, Nagoya University, Nagoya, Aichi 464-8602, Japan

Zong-Hong Zhu*

*School of Physics and Technology, Wuhan University, Wuhan, Hubei 430072, China and
Department of Astronomy, Beijing Normal University, Beijing 100875, China*

(Dated: September 18, 2020)

The coherent nature of gravitational wave emanating from a compact binary system makes it possible to detect some interference patterns in two (or more) signals registered simultaneously by the detector. Gravitational lensing effect can be used to bend trajectories of gravitational waves, which might reach the detector at the same time. Once this happens, a beat pattern may form, and can be used to obtain the luminosity distance of the source, the lens mass, and cosmological parameters such as the Hubble constant. Crucial question is how many such kind of events could be detected. In this work, we study this issue for the future space-borne detectors: DECIGO and its downscale version, B-DECIGO. It is found out that there can be a few tens to a few hundreds of lensed gravitational wave events with the beat pattern observed by DECIGO and B-DECIGO per year, depending on the evolution scenario leading to the formation of double compact objects. In particular, black hole-black hole binaries are dominating population of lensed sources in which beat patterns may reveal. However, DECIGO could also register a considerable amount of lensed signals from binary neutron stars, which might be accompanied by electromagnetic counterparts. Our results suggest that, in the future, lensed gravitational wave signal with the beat pattern could play an important role in cosmology and astrophysics.

I. INTRODUCTION

Einstein's prediction of gravitational waves (GWs) [1] has been verified by the detection of GWs by LIGO/Virgo Collaborations [2]. These observations marked the new era of GW astronomy and multimessenger astrophysics [2, 3]. Together with its electromagnetic counterpart, the GW could shed new light on cosmology, since its source can be used as the standard siren to accurately measure the luminosity distance [4]. It is also interesting to know that it may not be necessary to rely on the electromagnetic counterpart to determine the redshift of the source as discussed in Refs. [5–8]. The GW can also serve as a probe into fundamental physics [9], such as the nature of gravity [10] and spacetime [11].

The GW travels at the speed of light in vacuum c (i.e. along null geodesic) as predicted by general relativity [12]. If there is a massive enough object near its path, the trajectory of the GW is bent due to the curvature of spacetime produced by this object. This is the gravitational lensing effect [13, 14]. Although the light can also be gravitationally lensed, one should understand that there are several differences between the lensing of the light and that of the GW. First, GWs usually have much longer wavelengths than the light. Second, the GW produced by a compact binary system is nearly monochromatic, so it is coherent; in contrast, the light emitted by a star is incoherent. Because of the long wavelengths of GWs, the lens should be very massive in order for the geometric optics to be applicable. For example, the mass of the lens should be greater than $10^4 M_\odot$ for the ground-based detectors, which are operating in the frequency range $1 \sim 10^4$ Hz; for LISA (frequency

* zhuzh@whu.edu.cn

range $10^{-4} \sim 0.1$ Hz), the lens should be $10^8 M_\odot$, at least [15, 16]. Although we will refer to the wave nature of GWs, we focus on the geometric optics regime. In this regime, the lensed GW has magnified amplitude and its polarization plane gets rotated [17]. However, the deflection angle is very small, so the rotation of the polarization plane can be ignored.

As an effect of the gravitational lensing, there can be multiple paths along which GWs reach the detector. The GWs along different paths experience distinct gravitational time dilation, and the lengths of the paths are not the same, so there exist time delays Δt between them [13]. If it happens that, during some time window, the interferometer simultaneously detects the GWs coming from the same source along different trajectories, interference patterns may occur [18, 19]. During the inspiral phase, frequency of the GW evolves very slowly. Consequently, there might be a small frequency difference Δf between the GWs coming from the lensed images of the source. Therefore, if Δf is small enough the interference results in a beat pattern, which can be used to extract useful information (e.g., lensing time delay Δt and the magnifications) and further to measure the true luminosity distance of the source, the lens mass, and cosmological parameters as discussed in Ref. [19]. In typical cases of galaxy lensing, time delay Δt might be of order of a few days to a few months. Therefore, it is highly impossible for a ground-based detector operating at high frequencies to simultaneously observe the lensed GWs traveling along different paths. This is because the GW from the final merger phase detectable in the frequency range of the ground-based detector lasts for a few hundred seconds at most. However, there is no difficulty for the space-borne detector sensitive to low GW frequencies to observe the beat pattern. Therefore, it is very interesting to study the prospects of future space-borne GW detectors to register the beat patterns from lensed GW signals.

As a starting point, one should estimate how many lensed GW events exhibiting the beat pattern to be detected by the space-borne detector per year. If the detection rate is large enough, it would definitely be important to study such phenomenon further. In the past, Sereno *et al.* calculated the number of lensed GW events that might be observed by LISA [20]. They found out that there can be at most 4 lensed GW events in a 5-year mission. Since they did not specialize the particular events with the beat pattern, one expects that those with the beat pattern should be fewer than 4. Nevertheless, it is worth to note that even with such a low detection rate, some interesting constraints on cosmological parameters can still be derived according to Ref. [21]. One expects that with a higher detection rate, the constraints can be improved. The low detection rate is related to the fact that the number of the massive black hole binaries, the main targets of LISA, is only on the order of 10^3 [22, 23]. On the contrary, there are many more less massive compact binaries, whose merger rate is larger by a few or-

ders of magnitude [2, 24, 25]. These mergers might be easier detected by a second space-borne interferometer, DECi-hertz Interferometer Gravitational wave Observatory (DECIGO) [5, 26, 27].

DECIGO is a planned Japanese space-borne interferometer, which is sensitive to GWs at mHz to 100 Hz. Since its sensitive band is higher than that of LISA, DECIGO is capable of observing GWs from much less massive binaries. Moreover, some of these binaries would also be targets of ground-based detectors, such as LIGO/Virgo and Einstein Telescope (ET) [28]. Therefore, DECIGO and ground based detectors can observe some merging binary systems jointly (but at different times, of course) to make the multiband GW astronomy possible [29]. Like the LISA Pathfinder, a downscale version of DECIGO, B-DECIGO, will also be operating in the similar frequency band, but will be less sensitive [30, 31]. In this work, we discuss the detection rates of the lensed GW events exhibiting the beat pattern observable by (B-)DECIGO.

The predictions of the GW lensing rate have been formulated by several authors for different interferometers. As mentioned above, Sereno *et al.* estimated how many lensed GW events can be detected by LISA [20]. For ground-based detectors, Ref. [32] predicted that there would be only 1 lensed GW event per year for aLIGO at its design sensitivity, but ET can detect about 80 events. Refs. [33–37] all discussed the lensing rate for ET, and concluded that there are $50 \sim 100$ events per year. Recently, Ref. [38] predicted the lensing rates for (B-)DECIGO, but the possibility of the beat pattern was not considered. This work will fill in the gap.

Gravitational lensing has many applications other than those discussed in Ref. [19]. For instance, one can detect dark matter [39–43], constrain the speed of light [44, 45], determine the cosmological constant [20, 21, 46], examine the wave nature of GWs [47–49], and localize the host galaxies of strong lensed GWs [50, 51] using gravitational lensing. Although no gravitational lensing signals have been detected in the observed GW events, the advent of more sensitive GW detectors might make it possible soon [52].

This work is organized in the following way. We will start with a brief review of the formation of the beat pattern due to the lensing effect in Sec. II. Then, (B-)DECIGO will be introduced in Sec. III. Section IV discusses the lens model and how to calculate the optical depth, and the lensing rates are computed in Sec. V. In the end, there is a short conclusion in Sec. VI. We choose a units such that $c = 1$.

II. THE BEAT PATTERN

In this section, we shall briefly review the formation of the beat pattern due to the gravitational lensing effect of GWs. For more detail, please refer to Ref. [19].

We will assume that the lens is described by a singular isothermal sphere (SIS), which models the early

type galaxies, because the early type galaxies contribute to the strong lensing probability dominantly [53]. The line-of-sight velocity dispersion σ_v of stars in the galaxy characterizes the lensing effect. As shown in Fig. 1, the GW produced by the source S can travel in two paths, labeled by 1 and 2, to arrive at the observer O due to the presence of a lens L. β is the misalignment angle between the optical axis OL and the would-be viewing direction OS if there were no lens. Deflected rays form two angles, θ_{\pm} , with OL at the observer, which are given by [13]

$$\theta_{\pm} = \beta \pm \theta_E, \quad (1)$$

where $\theta_E = 4\pi\sigma_v^2 D_{LS}/D_S$ is the angular Einstein radius, and D_{LS} and D_S are the angular diameter distances indicated in the Fig. 1. In further considerations concerning merger rates we will assume flat Λ CDM model, in which the angular diameter distance $D_A(z)$ between the Earth and a celestial object at the redshift z is [54]

$$D_A(z) = \frac{1}{H_0(1+z)} \int_0^z \frac{dz'}{h(z')} \quad (2)$$

where H_0 is the Hubble constant, $h(z) = [\Omega_m(1+z)^3 + \Omega_{\Lambda}]^{1/2}$ is the dimensionless expansion rate. In order to comply with population synthesis model used further in this paper, we assume $\Omega_m = 0.3$ and $H_0 = 70 \text{ km s}^{-1} \text{ Mpc}^{-1}$. Therefore, in our shorthand notation: $D_L = D_A(z_L)$, and $D_S = D_A(z_S)$ with z_L and z_S the redshifts of the lens and the source, respectively. $D_{LS} = \frac{1}{H_0(1+z_S)} \int_{z_L}^{z_S} \frac{dz'}{h(z')}$ is the angular diameter distance between the lens and the source.

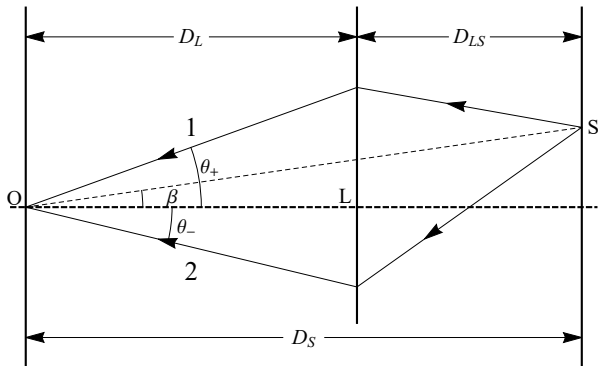


FIG. 1. The geometry of a lens. Two GW rays, 1 and 2, originating from the source S, travel along two trajectories and change their directions near the lens L. Eventually, they arrive at the detector at O. Vertical lines represent the observer, lens and source planes, from the left to the right. Thick dashed line is the optical axis, and the thin dashed line would be the viewing direction if there were no lens. The angle between the two dashed lines is called the misalignment angle β . The GW rays form the angles θ_+ and θ_- with the optical axis at the observer. The distances D_S , D_L , and D_{LS} are angular diameter distances.

Lensed GW signals are magnified, and the magnifica-

tion factors of the GW amplitudes are given by

$$\mu_{\pm} = \sqrt{\left| \frac{\theta_{\pm}/\theta_E}{|\theta_{\pm}/\theta_E| - 1} \right|}. \quad (3)$$

Finally, the GW rays travel along paths of different lengths, and they experience different time dilation due to the gravitational potential of the lens, so they arrive at the observer at different times. The time delay is

$$\Delta t = 32\pi^2 \sigma_v^4 (1+z_L) \frac{D_L D_{LS}}{D_S} \frac{\beta}{\theta_E}. \quad (4)$$

One can see that σ_v , appearing in Eqs. (1), (3), and (4), indeed characterizes the lensing effect of a SIS model.

The time delay Δt typically ranges from a few days to a few months. For example, one can assume that the GW source is at $z_S = 2$, and the lens at $z_L = 1$. Such value of z_S is suggested by the fact that the redshift distribution of detectable neutron star-neutron star mergers (NS-NS) is maximal near $z = 2$, the redshift of black hole-black hole mergers (BH-BH) peaks around $z = 4$ [37] and the lensing probability is maximal roughly for a lens halfway between the source and observer. Taking σ_v as a characteristic velocity dispersion $\sigma_* = 161 \pm 5 \text{ km/s}$ [55], then $2.03 \text{ weeks} < \Delta t < 1.18 \text{ months}$ for $0.1 \text{ arcsecond} < \beta < 0.25 \text{ arcsecond}$. Note that $\beta < \theta_E \approx 0.27 \text{ arcsecond}$ in order that the interferometer can “hear” two GWs.

One can reasonably expect that Δt is much longer than the duration of GW signal observed by ground-based interferometers. Of course, one may imagine a case where β is very small, of the order of $10^{-5} - 10^{-7} \text{ arcsecond}$, such that $\Delta t \sim$ is of order of a few seconds, and the beat pattern forms, as displayed in Fig. 2 in Ref. [19]. But the probability for such case is extremely low. Therefore, it is very unlikely to use ground-based interferometers to observe the interference patterns in GW events lensed by a SIS. However, the signals observed by LISA and (B-)DECIGO usually last for several months or even years. So, there is no difficulty for them to simultaneously detect two lensed GW signals in some time window. These signals would interfere with each other and form an interference pattern in the time domain. If the strains for the lensed GWs are $h_1(t)$ and $h_2(t)$, the total strain is simply

$$h(t) = h_1(t) + h_2(t). \quad (5)$$

Suppose the frequencies of h_1 and h_2 are f_1 and f_2 , respectively. Without the loss of generality, let $f_1 > f_2$, i.e., we assume h_1 arrives earlier than h_2 . Their difference $\Delta f = f_1 - f_2$ is much smaller than both f_1 and f_2 in the inspiral phase, due to slow evolution of the GW frequency during the lensing time delay. Therefore, the beat pattern could show up during the inspiral phase, as discussed in Ref. [19]. As the binary system evolves, the GW frequency increases, so the beat pattern has a smaller and smaller period. Eventually, the beat pattern disappears, and a generic interference pattern is left.

Taking into account the orbital motion of the spaceborne interferometer, the beat pattern would have more complicated behavior than that described above. So one may want to consider the cases with small enough Δt such that the impact on the beat pattern due to the changing orientation of the constellation plane is small enough, and the analysis is easier. Of course, Δt should not be too small; otherwise, the probability for such events would be negligible again. So in this work, we would like to mainly consider the lensing events with $\Delta t = 1$ month.

The Fourier transformation of the strain is used to calculate the signal-to-noise ratio (SNR). Let $h_1(t)$ be Fourier transformed to

$$\begin{aligned}\tilde{h}_1(f) &= \mu_+ \int_{-\infty}^{\infty} h_u(t) e^{i2\pi f t} df \\ &= \mu_+ \tilde{h}_u(f),\end{aligned}\quad (6)$$

where $h_u(t)$ would be the strain if there were no lens, and $\tilde{h}_u(f)$ is its Fourier transform. Then the frequency domain waveform $\tilde{h}_2(f)$ for $h_2(t) = \frac{\mu_-}{\mu_+} h_1(t - \Delta t)$ is

$$\tilde{h}_2(f) = e^{i2\pi f \Delta t} \mu_- \tilde{h}_u(f). \quad (7)$$

So the amplitude of the total waveform is

$$|\tilde{h}(f)| = \sqrt{\mu_+^2 + \mu_-^2 + 2\mu_+\mu_- \cos(2\pi f \Delta t)} |\tilde{h}_u(f)|. \quad (8)$$

This suggests that in the frequency domain, the amplitude of the total waveform is also oscillating with a ‘‘period’’ $1/\Delta t$.

III. DECIGO AND B-DECIGO

In this work, we estimate the lensing rate of lensed GW events with beat patterns detectable by (B-)DECIGO, so this section briefly reviews the detectors characteristics. DECIGO is supposed to have a configuration of four clusters of spacecrafts. Each cluster would consist of three drag-free satellites, separated from each other by 1000 km and forming an equilateral triangle. All four clusters would orbit around the Sun with a period of 1 yr. DECIGO was originally proposed in Ref. [5]. Over the following years, it evolved somehow, and now, its current objectives and design can be found in Ref. [27, 31].

According to Yagi & Seto [56], a triangular cluster is equivalent to two L-shaped interferometers rotated by 45° with uncorrelated noise. The noise spectrum for a single effective L-shape DECIGO is

$$\begin{aligned}S_h(f) &= 10^{-48} \times \left[7.05 \left(1 + \frac{f^2}{f_p^2} \right) + 4.80 \times 10^{-3} \times \right. \\ &\quad \left. \frac{f^{-4}}{1 + (f/f_p)^2} + 5.33 \times 10^{-4} f^{-4} \right] \text{ Hz}^{-1},\end{aligned}\quad (9)$$

where $f_p = 7.36$ Hz.

B-DECIGO is the ‘‘DECIGO Pathfinder’’, and has only one cluster of spacecrafts. The distance between spacecrafts is also smaller, which is 100 km. Its sensitivity is of course lower and can be described by the following effective noise spectrum [57],

$$\begin{aligned}S_h(f) &= 10^{-46} \times [4.040 + 6.399 \times 10^{-2} f^{-4} \\ &\quad + 6.399 \times 10^{-3} f^2] \text{ Hz}^{-1}.\end{aligned}\quad (10)$$

Fig. 2 shows the characteristic strains $\sqrt{f S_h}$ for these two detectors. For comparison, the signals of GW150914 and GW170817 are also plotted, using PyCBC [58]. Although

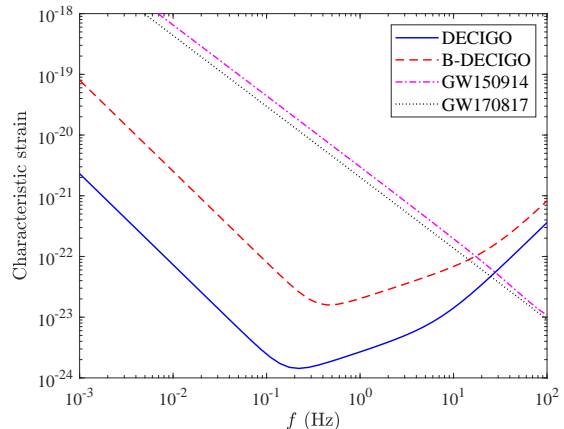


FIG. 2. Characteristic strains of for DECIGO (solid blue curve) and B-DECIGO (dashed red curve). The dot-dashed and the dotted curves are signals of GW150914 and GW170817, respectively.

not shown in this figure, both of the two signals will later end with a merger well beyond the sensitivity bands of (B-)DECIGO, but accessible to LIGO/Virgo and definitely also to next generation of ground-based detectors.

As one can see, both GW150914 and GW170817 would be detected by (B-)DECIGO in their inspiral phase. So if GW150914, for instance, were gravitationally lensed with a one-month time delay, then one may observe the beat pattern shown in Fig. 3. This figure displays the beat pattern (the black curve) formed due to the interference between two GW rays (the blue and the red curves) traveling in different paths because of a suitable SIS lens. Here, for the purpose of demonstration, we only consider the quadruple contribution to the waveform, and assume the GWs incident the detector nearly perpendicularly and the inclination angle is zero.

Once one knows the Fourier transform $\tilde{h}(f)$ of a signal $h(t)$, one can calculate the SNR ρ of it [59],

$$\rho^2 = 4 \int_0^\infty \frac{|\tilde{h}(f)|^2}{S_h(f)} df. \quad (11)$$

If $\rho > \rho_{\text{th}}$, a threshold SNR, one may claim a detection of the GW. This condition may not necessarily mean one

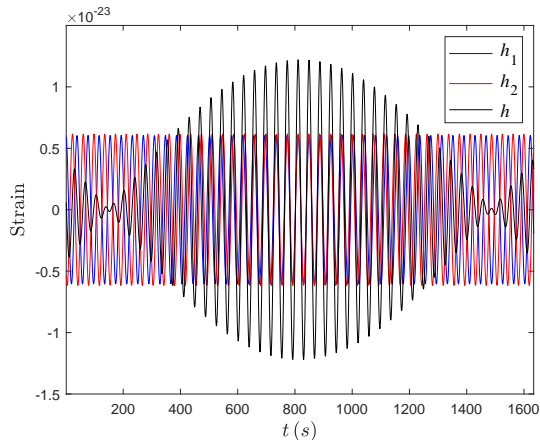


FIG. 3. A schematic diagram showing the time domain waveform of the beat pattern. The binary system is assumed to be GW150914, and the GW is gravitationally lensed by a suitable SIS lens. The time delay is assumed to be 1 month. The blue and the red curves are for the strains of the GW rays propagating in two different trajectories, and the black curve is for the interfered wave.

can easily extract some useful information from the beat pattern. For that purpose, one expects that the higher the SNR is, the easier the extraction can be done. However, we will not determine the least SNR for an accurate extraction in this work, in spite of its importance.

IV. THE LENS MODEL AND THE OPTICAL DEPTH

The lens model is chosen to be the SIS. The elementary cross section for lensing is [21]

$$s_{cr} = 16\pi^3\sigma^4 \left(\frac{D_L D_{LS}}{D_S} \right)^2 (y_{\max}^2 - y_{\min}^2). \quad (12)$$

Here, $y = \beta/\theta_E$, and y_{\max} is its maximal value, determined by requirement that lensed GW signals could be detected as displaying the beat pattern. Concerning the minimal value, arising when the geometric optics approximation breaks down, we assume $y_{\min} = 0$ as suggested by Ref. [21]. To determine y_{\max} , one first notes that $y_{\max} \leq 1$ [13]. Second, the observed SNR of the GW signal ρ should be greater than a threshold usually assumed as $\rho_{\text{th}} = 8$. This might be too low to extract useful information from the beat pattern. However, for our purpose it would be sufficient to assume this standard threshold. It can be easily adjusted in the following calculations. Third, the time delay $\Delta t = y\Delta t_z$, with [20]

$$\Delta t_z \equiv 32\pi^2\sigma^4 \frac{D_L D_{LS}}{D_S} (1 + z_L). \quad (13)$$

should be small enough, say less than $\Delta t_m = 1$ month. Now, according to Eqs. (8) and (11), one knows that

$$\rho^2 = 4 \int_0^\infty \frac{\mu_+^2 + \mu_-^2 + 2\mu_+\mu_- \cos(2\pi f \Delta t)}{S_h(f)} |\tilde{h}_u(f)|^2 df. \quad (14)$$

The cosine term in the integrand is highly oscillating compared to $|\tilde{h}_u(f)|$ in the frequency domain, so one may ignore it for the purpose of estimating the lensing rate, and the total GW SNR is $\rho \approx \sqrt{\mu_+^2 + \mu_-^2} \rho_{\text{int}} = \sqrt{2/y} \rho_{\text{int}}$ with ρ_{int} the intrinsic SNR,

$$\rho_{\text{int}} = 4 \int_0^\infty \frac{|\tilde{h}_u(f)|^2}{S_h(f)} df. \quad (15)$$

Therefore, one has

$$y_{\max} = \min \left\{ y_1, \frac{\Delta t_m}{\Delta t_z} \right\}, \quad (16)$$

with $y_1 = \min\{1, 2\rho_{\text{int}}^2/\rho_{\text{th}}^2\}$.

Since (B-)DECIGO will operate for a limited amount of time, the actual cross section used to calculate the optical depth is [21]

$$s_{cr}^* = 16\pi^3 \left(\frac{\sigma}{c} \right)^4 \left(\frac{D_L D_{LS}}{D_S} \right)^2 \left(y_{\max}^2 - \frac{2\Delta t_z}{3T_s} y_{\max}^3 \right), \quad (17)$$

where T_s is the survey time, and set to 4 years [38]. The differential optical depth is given by [20]

$$\frac{\partial^2 \tau}{\partial z_L \partial \sigma} = \frac{dn}{d\sigma} s_{cr}^* \frac{dt}{dz_L}, \quad (18)$$

where τ is the optical depth, z_L is the redshift of the lens, n is the lens number density, t is the cosmological time and $dn/d\sigma$ is modeled as a modified Schechter function [55]

$$\frac{dn}{d\sigma} = \frac{n_*}{\sigma_*} \frac{\beta}{\Gamma(\alpha/\beta)} \left(\frac{\sigma}{\sigma_*} \right)^{\alpha-1} \exp \left[- \left(\frac{\sigma}{\sigma_*} \right)^\beta \right] \quad (19)$$

where $\Gamma(x)$ is the gamma function, and

$$n_* = 8.0 \times 10^{-3} h^3 \text{ Mpc}^{-3}, \quad \sigma_* = 161 \pm 5 \text{ km/s}, \quad (20)$$

$$\alpha = 2.32 \pm 0.10, \quad \beta = 2.67 \pm 0.07. \quad (21)$$

Further, by the definition of the redshift [54],

$$1 + z = \frac{a_0}{a}, \quad (22)$$

one can determine the final factor in Eq. (18), which is

$$\frac{dt}{dz_L} = - \frac{1}{(1 + z_L)H_L}, \quad H_L = H(z_L). \quad (23)$$

So now, one can calculate the differential optical depth $d\tau/dz_L$ using Eq. (18),

$$\frac{d\tau}{dz_L} = \int_0^\infty \frac{\partial^2 \tau}{\partial z_L \partial \sigma} d\sigma. \quad (24)$$

The complexity of Eqs. (16) and (18) makes the above integration very difficult. But since Δt_z is an increasing function of σ according to (13), there exists a value σ_1 such that if $\sigma < \sigma_1$, $y_{\max} = y_1$, while if $\sigma \geq \sigma_1$, $y_{\max} =$

$\Delta t_m/\Delta t_z$. This σ_1 is given by

$$\sigma_1 = \left[\frac{\Delta t_m}{32\pi^2 y_1} \frac{D_S}{D_L D_{LS}} \frac{1}{1+z_L} \right]^{1/4}, \quad (25)$$

obtained from the condition $y_1 = \Delta t_m/\Delta t_z$. Then, one can carry out the integration (24) by dividing the integration range into two parts, separated by σ_1 . This gives

$$\begin{aligned} \frac{d\tau}{dz_L} = & \frac{16\pi^3 y_1^2 n_*}{\Gamma(\alpha/\beta)} \left(\frac{\sigma_*}{c}\right)^4 \frac{c(1+z_L)^2}{H_L} \left(\frac{D_L D_{LS}}{D_S}\right)^2 \left[\Gamma\left(\frac{\alpha+4}{\beta}\right) \mathcal{P}\left(u_1, \frac{\alpha+4}{\beta}\right) - \frac{2\Delta t_* y_1}{3T_s} \times \right. \\ & \left. \Gamma\left(\frac{\alpha+8}{\beta}\right) \mathcal{P}\left(u_1, \frac{\alpha+8}{\beta}\right) \right] + \frac{(c\Delta t_m)^2 n_*}{64\pi\Gamma(\alpha/\beta)} \left(\frac{c}{\sigma_*}\right)^4 \frac{c}{H_L} \left(1 - \frac{2\Delta t_m}{3T_s}\right) \mathcal{Q}\left(u_1, \frac{\alpha-4}{\beta}\right), \end{aligned} \quad (26)$$

where Δt_* is given by Eq. (13) with σ replaced by σ_* , $u_1 = (\sigma_1/\sigma_*)^\beta$, and

$$\mathcal{P}(x, a) = \frac{1}{\Gamma(a)} \int_0^x \xi^{a-1} e^{-\xi} d\xi, \quad (27)$$

$$\mathcal{Q}(x, a) = \int_x^\infty \xi^{a-1} e^{-\xi} d\xi, \quad (28)$$

are the incomplete gamma functions. The optical depth is thus

$$\tau(z_S) = \int_0^{z_S} \frac{d\tau}{dz_L} dz_L. \quad (29)$$

This integration can be performed numerically.

V. LENSING RATES

In this section, we will estimate the yearly detection rate of lensed GW events displaying the beat pattern. We consider GWs emitted by the double compact objects (DCOs), which include NS-NS, black hole-neutron star binaries (BH-NS) and BH-BH. Following Ref. [35], we use the intrinsic coalescence rate $\dot{n}_0(z)$ for DCOs in the local universe discussed in Ref. [60] and the data (more specifically, the so-called “rest frame rates” in cosmological scenario) from the website <https://www.syntheticuniverse.org/>. The intrinsic rate $\dot{n}_0(z)$ was calculated based on well-motivated assumptions about star formation rate, galaxy mass distribution, stellar populations, their metallicities and galaxy metallicity evolution with redshift (“low-end” and “high-end” cases). The binary system evolves from zero-age main sequence to the compact binary formation after supernova (SN) explosions. Since the formation of the compact object is related to the physics of common envelope (CE) phase of evolution and on the SN explosion mechanism, and both of them are uncertain to some extent, Ref. [60] considered four scenarios: standard one – based

on conservative assumptions, and three of its modifications — Optimistic Common Envelope (OCE), delayed SN explosion and high BH kicks scenario. For more details, see [60] and references therein. The chirp masses are assumed: $1.2M_\odot$ for NS-NS, $3.2M_\odot$ for BH-NS, and $6.7M_\odot$ for BH-BH. These values are the average chirp masses for these different binary systems given by the population synthesis [61]. The median chirp masses used in previous papers according to [61] were: $1.2M_\odot$ for NS-NS, $3.2M_\odot$ for BH-NS, and $6.7M_\odot$ for BH-BH. However, these were values obtained under the assumption of solar metallicity of initial binary systems. Such scenario was absolutely right guess before the first detections of GWs. Now, the data gathered by the LIGO/Virgo detectors have significantly modified these guesses demonstrating that observed chirp masses (pticular of BH-BH systems) are much higher. Therefore, guided by the real data gathered so far we will adopt different values. According to [2] we will assume the median value of BH-BH systems chirp masses reported in their Table III. Since the data on BH-NS systems is more scarce, we will take the value of [2]. In summary, we take the following values as representative of typical chirp masses of DCO inspiralling systems: $1.2 M_\odot$ for NS-NS, $6.09 M_\odot$ for BH-NS, and $24.5 M_\odot$ for BH-BH.

Matched filtering is used to identify GW events. The SNR for a single detector can be approximately determined with [62]

$$\rho = 8\Theta \frac{r_0}{d_L(z_S)} \left(\frac{\mathcal{M}_z}{1.2M_\odot}\right)^{5/6} \sqrt{\zeta(f_{\max})}, \quad (30)$$

where Θ is the orientation factor, $\mathcal{M}_z = (1+z_S)\mathcal{M}_0$ is the chirp mass registered by the detector, \mathcal{M}_0 is the chirp mass at the source frame, $d_L(z_S)$ is the luminosity distance, and finally, r_0 is the detector’s characteristic distance. The function $\zeta(f_{\max})$ is

$$\zeta(f_{\max}) = \frac{1}{x_{7/3}} \int_0^{2f_{\max}} \frac{(\pi M_\odot)^2}{(\pi M_\odot f)^{7/3} S_h(f)} df, \quad (31)$$

where $x_{7/3}$ is nothing but the above integration with the upper limit being infinity. Since DCO inspiralling systems studied in this work pass the sensitivity bands of (B-)DECIGO, one assumes that $\zeta(f_{\max}) = 1$ [38]. The characteristic distance parameter r_0 is determined by

$$r_0^2 = \frac{5}{192\pi^{4/3}c^3} \left(\frac{3GM_\odot}{20} \right)^{5/3} \int_0^\infty \frac{df}{f^{7/3}S_h(f)}. \quad (32)$$

From this, one finds out that $r_0 = 6709$ Mpc for DE-CIGO, and $r_0 = 535$ Mpc for B-DECIGO.

The orientation factor Θ is defined as

$$\Theta = 2\sqrt{F_+^2(1 + \cos^2 \iota)^2 + 4F_\times^2 \cos^2 \iota}, \quad (33)$$

where F_+ and F_\times are the antenna pattern functions for the + and \times polarizations, respectively, given by [63]

$$F_+ = \frac{1}{2}(1 + \cos^2 \theta) \cos 2\phi \cos 2\psi - \cos \theta \sin 2\phi \sin 2\psi, \quad (34)$$

$$F_\times = \frac{1}{2}(1 + \cos^2 \theta) \cos 2\phi \sin 2\psi + \cos \theta \sin 2\phi \cos 2\psi. \quad (35)$$

In these expressions, θ and ϕ are the polar and azimuthal angles of the spherical coordinate system, which centers at the detector and whose z -axis is perpendicular to the detector plane. ι is the inclination angle between the GW propagation direction and the angular momentum of the binary system, and finally, ψ is called the polarization angle. These angles ($\theta, \phi, \iota, \psi$) are uncorrelated and uniformly distributed, so the probability distribution $P(\Theta)$ of Θ is approximated by [64]

$$P(\Theta) = \frac{5\Theta(4 - \Theta)^3}{256}, \quad (36)$$

for $0 < \Theta < 4$, and $P(\Theta) = 0$, otherwise.

The differential beat rate is given by [35]

$$\frac{\partial^2 \dot{N}}{\partial z_S \partial \rho} = \frac{4\pi \dot{n}_0(z_S) d_L^2(z_S)}{(1 + z_S)^3 H(z_S)} \tau(z_S) P_\Theta(x(z_S, \rho)) \frac{x(z_S, \rho)}{\rho}, \quad (37)$$

where

$$x(z, \rho) = \frac{\rho}{\rho_{\text{th}}} (1 + z)^{-5/6} \frac{d_L(z)}{r_0} \left(\frac{1.2M_\odot}{\mathcal{M}_0} \right)^{5/6}. \quad (38)$$

The yearly detection rate is thus

$$\dot{N} = \int_0^{z_{\max}} dz_S \int_0^\infty d\rho \frac{\partial^2 \dot{N}}{\partial z_S \partial \rho}, \quad (39)$$

and the differential yearly detection rates are defined to be

$$\frac{\partial \dot{N}}{\partial \rho} = \int_0^{z_{\max}} dz_S \frac{\partial^2 \dot{N}}{\partial z_S \partial \rho}, \quad (40)$$

$$\frac{\partial \dot{N}}{\partial z_S} = \int_0^\infty d\rho \frac{\partial^2 \dot{N}}{\partial z_S \partial \rho}. \quad (41)$$

Figure 4 shows the relative differential detection rates $\frac{1}{\dot{N}} \frac{\partial \dot{N}}{\partial \rho}$ v.s. ρ for (B-)DECIGO. The evolutionary model for DCOs is the standard one with the “low-end” metallicity scenario. As one can see low SNR events of three different types of DCOs dominate for B-DECIGO. For DECIGO, although the relative differential rate for NS-NS type DCOs peaks at a small SNR ($\rho < \rho_{\text{th}}$), the curves for the remaining types of DCOs are more flat and reach maximum at higher SNRs.

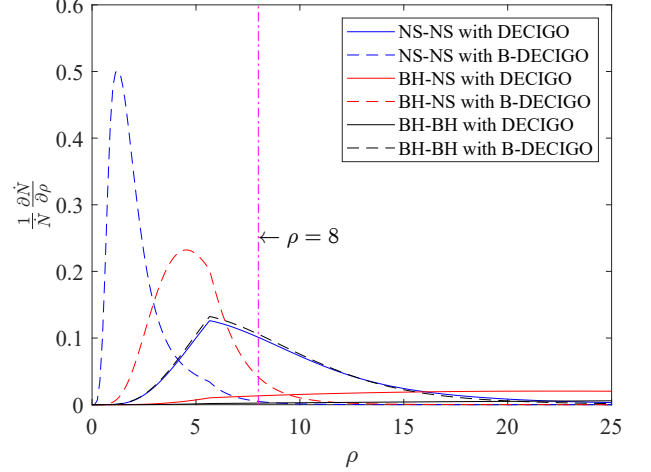


FIG. 4. The relative differential detection rates $\frac{1}{\dot{N}} \frac{\partial \dot{N}}{\partial \rho}$ v.s. ρ for (B-)DECIGO. The evolutionary model for DCOs is the standard one with the “low-end” metallicity scenario. The purple dot-dashed line is at $\rho = 8$.

Figure 5 displays the relative differential detection rates $\frac{1}{\dot{N}} \frac{\partial \dot{N}}{\partial z_S}$ v.s. z_S for (B-)DECIGO. The evolutionary model for DCOs is also the standard one with the “low-end” metallicity scenario. From this figure, one can see that lensed GW events observable in DECIGO are dominated by NS-NS and BH-NS binaries at $z_S = 2 \sim 4$ and BH-BH binaries at $z_S = 4 \sim 5$. On the other hand, differential lensing rates for B-DECIGO peak at the slightly lower redshifts, respectively. The earlier launch of B-DECIGO would provide valuable information.

Table I displays the yearly detection rate \dot{N} for lensed GW events with the beat pattern from the inspiraling DCOs of different classes. As shown in the table, we consider all four scenarios with both the low-end and high-end metallicity evolution assumed. From this table, one finds out that lensed GWs generated by BH-BH binary systems dominate in most cases, except for the High BH kicks scenario, for which lensed GWs from NS-NS binaries contribute the most. One interesting result is that in all cases, there are at least 10 lensed GW events with the beat pattern from the NS-NS binaries per year. This creates possibility that at least for some of them electromagnetic counterparts could be detected allowing to identify the host galaxy and measure the redshift. Hence, the cosmological parameters could be measured from them according to Ref. [19]. Of course, one should also try to

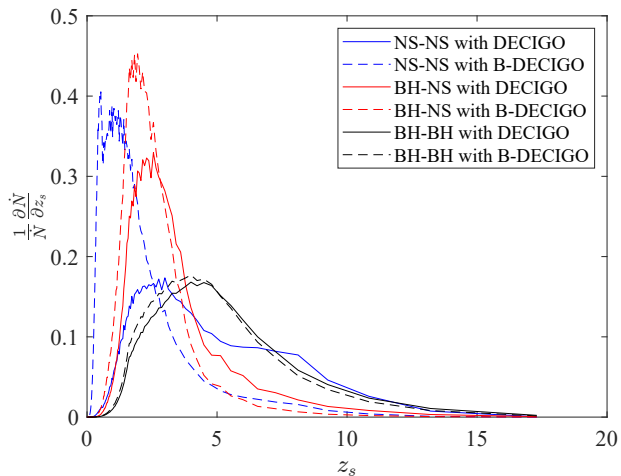


FIG. 5. The relative differential detection rates $\frac{1}{\dot{N}} \frac{\partial \dot{N}}{\partial z_s}$ v.s. z_s for (B-)DECIGO. The evolutionary model for DCOs is the standard one with the “low-end” metallicity scenario.

\dot{N}	Stand.	Opt. CE	Del. SN	BH kicks
NS-NS				
low-end metallicity	10.2	83.8	10.7	10.3
high-end metallicity	10.3	88.5	11.0	10.6
BH-NS				
low-end metallicity	5.9	9.5	2.9	0.7
high-end metallicity	5.1	9.5	2.5	0.6
BH-BH				
low-end metallicity	111.5	275.4	93.8	8.0
high-end metallicity	92.0	255.9	76.9	6.4
Total				
low-end metallicity	127.6	368.7	107.4	19.0
high-end metallicity	107.4	353.9	90.4	17.6

TABLE I. Yearly detection rate for lensed GW events exhibiting the beat pattern from inspiralling DCOs of different classes under different evolutionary scenarios, assuming “low-end” and “high-end” metallicity evolution. Predictions for DECIGO.

take advantage of the dominating BH-BH binary systems using statistical methods as discussed in Ref. [21].

Table II shows the yearly detection rate for lensed GW events with the beat pattern for B-DECIGO. Compared with Table I, it has similar features but the rates are smaller. This is due to the lower designed sensitivity. However, there is still a considerable amount of lensed events dominated by signals from BH-BH systems. The only exception is the High BH kicks scenario, leading to suppression of BH-BH formation rate. In such a case the perspectives for the B-DECIGO to detect lensed GW with a beat pattern are poor.

One may concern that in order to detect the beat patterns with enough accuracy to determine the luminosity distance, the lens mass and cosmological parameters,

\dot{N}	Stand.	Opt. CE	Del. SN	BH kicks
NS-NS				
low-end metallicity	0.05	0.63	0.06	0.06
high-end metallicity	0.09	0.59	0.10	0.09
BH-NS				
low-end metallicity	1.61	2.98	0.83	0.17
high-end metallicity	1.19	2.67	0.62	0.13
BH-BH				
low-end metallicity	82.8	216.7	69.0	5.65
high-end metallicity	66.6	197.7	55.14	4.43
Total				
low-end metallicity	84.46	220.3	69.89	5.88
high-end metallicity	67.88	201.0	55.86	4.65

TABLE II. Yearly detection rate for lensed GW events with the beat pattern from inspiralling DCOs of different classes under different evolutionary scenarios, assuming “low-end” and “high-end” metallicity evolution. Predictions for B-DECIGO.

SNR threshold ρ_{th} should be bigger than usually assumed value $\rho_{\text{th}} = 8$. It turns out, however, that by increasing ρ_{th} by a factor of 10 or even 100, the detection rates for the standard scenario case remain the same. This can be understood by realizing the fact that Eq. (39) can be rewritten in the following form,

$$\dot{N} = \int_0^{z_{\text{max}}} dz_s \int_0^\infty dR \frac{\partial^2 \dot{N}}{\partial z_s \partial R}, \quad (42)$$

where $R = \rho/\rho_{\text{th}}$, and the new integrand is given by replacing ρ by R in the denominator of the last factor in Eq. (37). According to Eq. (38), $x(z, \rho)$ is actually a function of R . Moreover, the optical depth $\tau(z_s)$ also depends on R ; see the definition of y_1 below Eq. (16), and also Eq. (26). Therefore, the new integrand $\frac{\partial^2 \dot{N}}{\partial z_s \partial R}$ is indeed a function of R , and \dot{N} is insensitive to the choice of ρ_{th} for any DCO evolutionary scenario.

VI. CONCLUSION

In this work, we analyzed how many lensed GW events with the beat pattern can be detected by (B-)DECIGO every year. It turns out that there are many more lensed events from DCOs than those observable by LISA [20]. Among different binary types of DCOs, BH-BH binaries contribution is dominating in most evolutionary models of DCOs. Nevertheless, there is still a considerable number of lensed GWs expected from NS-NS and BH-NS binaries, which can be used together with their electromagnetic counterparts to study the cosmology accurately. In fact, the lensed GWs from BH-BH binaries are also valuable with the statistics method [21], even though there are no electromagnetic counterparts.

Another point worth mentioning is that it is very advantageous to study cosmology with the beat pattern, because high redshift binaries ($z_S = 3 \sim 6$) contribute a lot to the total detection rates. In Ref. [19], the authors discussed how to use the beat pattern to measure the luminosity distance of the GW source, the mass of the lens, and some cosmological parameters (e.g., H_0). In principle, these measurements can be very accurate. However, these studies were based on the simple lens models: the point-mass model and SIS. One may expect that similar opportunity will emerge in more complicated and realistic lens mass profiles. This deserves further study. Moreover some complications arising in realistic situation were also omitted, such as the small SNRs for some GW events, the intrinsic scatter in the lens profile and the cosmic shear, etc.. One has to properly address these issues in the real measurements in order to guarantee accuracy of the method. In this work, we only estimate the lensing rate, which at the order of magnitude level would not be affected much by these factors. Our predic-

tions raise hopes of detecting beat patterns in forthcoming (B-)DECIGO missions and motivates to undertake more realistic studies of this phenomenon.

ACKNOWLEDGMENTS

This work was supported by the National Natural Science Foundation of China under Grants No. 11633001, No. 11673008, No. 11922303, and No. 11920101003 and the Strategic Priority Research Program of the Chinese Academy of Sciences, Grant No. XDB23000000. SH was supported by Project funded by China Postdoctoral Science Foundation (No. 2020M672400). HY was supported by Initiative Post-docs Supporting Program (No. BX20190206) and Project funded by China Postdoctoral Science Foundation (No. 2019M660085). MB was supported by the Key Foreign Expert Program for the Central Universities No. X2018002.

-
- [1] A. Einstein, Sitzungsber. Preuss. Akad. Wiss. Berlin (Math. Phys.) **1916**, 688 (1916); **1918**, 154 (1918).
- [2] B. P. Abbott *et al.* (Virgo and LIGO Scientific Collaborations), *Phys. Rev. Lett.* **116**, 061102 (2016), arXiv:1602.03837 [gr-qc]; *Phys. Rev. Lett.* **116**, 241103 (2016), arXiv:1606.04855 [gr-qc]; *Phys. Rev. Lett.* **118**, 221101 (2017), arXiv:1706.01812 [gr-qc]; *Phys. Rev. Lett.* **119**, 141101 (2017), arXiv:1709.09660 [gr-qc]; *Phys. Rev. Lett.* **119**, 161101 (2017), arXiv:1710.05832 [gr-qc]; *Astrophys. J.* **851**, L35 (2017), arXiv:1711.05578 [astro-ph.HE]; *Phys. Rev. X* **9**, 031040 (2019), arXiv:1811.12907 [astro-ph.HE]; *Astrophys. J. Lett.* **892**, L3 (2020), arXiv:2001.01761 [astro-ph.HE]; R. Abbott *et al.* (LIGO Scientific, Virgo), *Phys. Rev. D* **102**, 043015 (2020), arXiv:2004.08342 [astro-ph.HE]; *Astrophys. J. Lett.* **896**, L44 (2020), arXiv:2006.12611 [astro-ph.HE]; *Phys. Rev. Lett.* **125**, 101102 (2020), arXiv:2009.01075 [gr-qc]; *Astrophys. J. Lett.* **900**, L13 (2020), arXiv:2009.01190 [astro-ph.HE].
- [3] A. Goldstein *et al.*, *Astrophys. J.* **848**, L14 (2017), arXiv:1710.05446 [astro-ph.HE]; V. Savchenko *et al.*, *Astrophys. J.* **848**, L15 (2017), arXiv:1710.05449 [astro-ph.HE].
- [4] B. F. Schutz, *Nature* **323**, 310 (1986); D. E. Holz and S. A. Hughes, *Astrophys. J.* **629**, 15 (2005), arXiv:astro-ph/0504616 [astro-ph].
- [5] N. Seto, S. Kawamura, and T. Nakamura, *Phys. Rev. Lett.* **87**, 221103 (2001), arXiv:astro-ph/0108011 [astro-ph]; A. Nishizawa, K. Yagi, A. Taruya, and T. Tanaka, *Phys. Rev. D* **85**, 044047 (2012), arXiv:1110.2865 [astro-ph.CO]; C. Bonvin, C. Caprini, R. Sturani, and N. Tamanini, *Phys. Rev. D* **95**, 044029 (2017), arXiv:1609.08093 [astro-ph.CO].
- [6] C. Messenger and J. Read, *Phys. Rev. Lett.* **108**, 091101 (2012), arXiv:1107.5725 [gr-qc]; C. Messenger, K. Takami, S. Gossan, L. Rezzolla, and B. S. Sathyaprakash, *Phys. Rev. X* **4**, 041004 (2014), arXiv:1312.1862 [gr-qc].
- [7] S. Hou, X.-L. Fan, and Z.-H. Zhu, *Phys. Rev. D* **101**, 084052 (2020), arXiv:1911.04182 [gr-qc].
- [8] X. Ding, M. Biesiada, X. Zheng, K. Liao, Z. Li, and Z.-H. Zhu, *JCAP* **04**, 033 (2019), arXiv:1801.05073 [astro-ph.CO].
- [9] E. Barausse *et al.*, (2020), arXiv:2001.09793 [gr-qc].
- [10] A. Nishizawa, A. Taruya, K. Hayama, S. Kawamura, and M.-a. Sakagami, *Phys. Rev. D* **79**, 082002 (2009), arXiv:0903.0528 [astro-ph.CO]; C. M. Will, *Living Rev. Rel.* **17**, 4 (2014), arXiv:1403.7377 [gr-qc]; S. Hou, Y. Gong, and Y. Liu, *Eur. Phys. J. C* **78**, 378 (2018), arXiv:1704.01899 [gr-qc]; S. Hou and Y. Gong, *Universe* **4**, 84 (2018), arXiv:1806.02564 [gr-qc]; Y. Gong and S. Hou, *Universe* **4**, 85 (2018), arXiv:1806.04027 [gr-qc]; Y. Gong, S. Hou, D. Liang, and E. Papantonopoulos, *Phys. Rev. D* **97**, 084040 (2018), arXiv:1801.03382 [gr-qc]; S. Hou and Y. Gong, *Eur. Phys. J. C* **79**, 197 (2019), arXiv:1810.00630 [gr-qc]; M. Hohmann, L. Järv, M. Krššák, and C. Pfeifer, *Phys. Rev. D* **100**, 084002 (2019), arXiv:1901.05472 [gr-qc]; Y. Liu, W.-L. Qian, Y. Gong, and B. Wang, (2019), arXiv:1912.01420 [gr-qc].
- [11] D. Christodoulou, *Phys. Rev. Lett.* **67**, 1486 (1991); E. E. Flanagan and D. A. Nichols, *Phys. Rev. D* **95**, 044002 (2017), arXiv:1510.03386 [hep-th]; S. M. Du and A. Nishizawa, *Phys. Rev. D* **94**, 104063 (2016), arXiv:1609.09825 [gr-qc]; S. Hou and Z.-H. Zhu, (2020), arXiv:2005.01310 [gr-qc]; (2020), arXiv:2008.05154 [gr-qc].
- [12] C. W. Misner, K. S. Thorne, and J. A. Wheeler, *Gravitation* (W. H. Freeman, San Francisco, 1973).
- [13] P. Schneider, J. Ehlers, and E. E. Falco, *Gravitational Lenses* (Springer, Berlin, Heidelberg, 1992) p. 560.
- [14] J. K. Lawrence, *Il Nuovo Cimento B* (1971-1996) **6**, 225 (1971); *Phys. Rev. D* **3**, 3239 (1971).
- [15] M. Arnaud-Varvella, M. C. Angonin, and P. Tourrenc,

- Gen. Rel. Grav. **36**, 983 (2004), arXiv:gr-qc/0312028 [gr-qc].
- [16] A. K. Meena and J. S. Bagla, *Mon. Not. Roy. Astron. Soc.* **492**, 1127 (2019), arXiv:1903.11809 [astro-ph.CO].
- [17] S. Hou, X.-L. Fan, and Z.-H. Zhu, *Phys. Rev. D* **100**, 064028 (2019), arXiv:1907.07486 [gr-qc].
- [18] K. Yamamoto, *Phys. Rev. D* **71**, 101301(R) (2005), arXiv:astro-ph/0505116 [astro-ph].
- [19] S. Hou, X.-L. Fan, K. Liao, and Z.-H. Zhu, *Phys. Rev. D* **101**, 064011 (2020), arXiv:1911.02798 [gr-qc].
- [20] M. Sereno, A. Sesana, A. Bleuler, P. Jetzer, M. Volonteri, and M. C. Begelman, *Phys. Rev. Lett.* **105**, 251101 (2010), arXiv:1011.5238 [astro-ph.CO].
- [21] M. Sereno, P. Jetzer, A. Sesana, and M. Volonteri, *Mon. Not. Roy. Astron. Soc.* **415**, 2773 (2011), arXiv:1104.1977 [astro-ph.CO].
- [22] A. Sesana, M. Volonteri, and F. Haardt, *Laser Interferometer Space Antenna. Proceedings, 7th international LISA Symposium, Barcelona, Spain, June 16-20, 2008*, *Class. Quant. Grav.* **26**, 094033 (2009), arXiv:0810.5554 [astro-ph].
- [23] A. Klein *et al.*, *Phys. Rev. D* **93**, 024003 (2016), arXiv:1511.05581 [gr-qc].
- [24] D. Gerosa, S. Ma, K. W. K. Wong, E. Berti, R. O’Shaughnessy, Y. Chen, and K. Belczynski, *Phys. Rev. D* **99**, 103004 (2019), arXiv:1902.00021 [astro-ph.HE].
- [25] L. Boco, A. Lapi, S. Goswami, F. Perrotta, C. Baccigalupi, and L. Danese, *Astrophys. J.* **881**, 157 (2019), arXiv:1907.06841 [astro-ph.GA].
- [26] S. Kawamura *et al.*, *Laser interferometer space antenna. Proceedings, 8th International LISA Symposium, Stanford, USA, June 28-July 2, 2010*, *Class. Quant. Grav.* **28**, 094011 (2011).
- [27] S. Kawamura *et al.*, (2020), arXiv:2006.13545 [gr-qc].
- [28] M. Punturo *et al.*, *Gravitational waves. Proceedings, 8th Edoardo Amaldi Conference, Amaldi 8, New York, USA, June 22-26, 2009*, *Class. Quant. Grav.* **27**, 084007 (2010).
- [29] A. Sesana, *Phys. Rev. Lett.* **116**, 231102 (2016), arXiv:1602.06951 [gr-qc].
- [30] S. Sato *et al.*, *J. Phys.: Conf. Ser.* **840**, 012010 (2017).
- [31] S. Kawamura *et al.*, *Int. J. of Mod. Phys. D* **28**, 1845001 (2019).
- [32] S.-S. Li, S. Mao, Y. Zhao, and Y. Lu, *Mon. Not. Roy. Astron. Soc.* **476**, 2220 (2018), arXiv:1802.05089 [astro-ph.CO].
- [33] A. Piórkowska, M. Biesiada, and Z.-H. Zhu, *JCAP* **1310**, 022 (2013), arXiv:1309.5731 [astro-ph.CO].
- [34] M. Biesiada, X. Ding, A. Piórkowska, and Z.-H. Zhu, *JCAP* **10**, 080 (2014), arXiv:1409.8360 [astro-ph.HE].
- [35] X. Ding, M. Biesiada, and Z.-H. Zhu, *JCAP* **1512**, 006 (2015), arXiv:1508.05000 [astro-ph.HE].
- [36] M. Oguri, *Mon. Not. Roy. Astron. Soc.* **480**, 3842 (2018), arXiv:1807.02584 [astro-ph.CO].
- [37] L. Yang, X. Ding, M. Biesiada, K. Liao, and Z.-H. Zhu, *Astrophys. J.* **874**, 139 (2019), arXiv:1903.11079 [astro-ph.GA].
- [38] A. Piórkowska-Kurpas, S. Hou, M. Biesiada, X. Ding, S. Cao, X. Fan, S. Kawamura, and Z.-H. Zhu, (2020), arXiv:2005.08727 [astro-ph.HE].
- [39] C. Cutler and D. E. Holz, *Phys. Rev. D* **80**, 104009 (2009), arXiv:0906.3752 [astro-ph.CO].
- [40] S. Camera and A. Nishizawa, *Phys. Rev. Lett.* **110**, 151103 (2013), arXiv:1303.5446 [astro-ph.CO].
- [41] G. Congedo and A. Taylor, *Phys. Rev. D* **99**, 083526 (2019), arXiv:1812.02730 [astro-ph.CO].
- [42] S. Jung and C. S. Shin, *Phys. Rev. Lett.* **122**, 041103 (2019), arXiv:1712.01396 [astro-ph.CO].
- [43] K. Liao, X. Ding, M. Biesiada, X.-L. Fan, and Z.-H. Zhu, *Astrophys. J.* **867**, 69 (2018), arXiv:1809.07079 [astro-ph.CO].
- [44] X.-L. Fan, K. Liao, M. Biesiada, A. Piórkowska-Kurpas, and Z.-H. Zhu, *Phys. Rev. Lett.* **118**, 091102 (2017), arXiv:1612.04095 [gr-qc].
- [45] T. E. Collett and D. Bacon, *Phys. Rev. Lett.* **118**, 091101 (2017), arXiv:1602.05882 [astro-ph.HE].
- [46] K. Liao, X.-L. Fan, X.-H. Ding, M. Biesiada, and Z.-H. Zhu, *Nature Commun.* **8**, 1148 (2017), [Erratum: *Nature Commun.* 8, no.1, 2136(2017)], arXiv:1703.04151 [astro-ph.CO].
- [47] L. Dai, S.-S. Li, B. Zackay, S. Mao, and Y. Lu, *Phys. Rev. D* **98**, 104029 (2018), arXiv:1810.00003 [gr-qc].
- [48] K. Liao, M. Biesiada, and X.-L. Fan, *Astrophys. J.* **875**, 139 (2019), arXiv:1903.06612 [gr-qc].
- [49] D. Sun and X. Fan, (2019), arXiv:1911.08268 [gr-qc].
- [50] H. Yu, P. Zhang, and F.-Y. Wang, *Mon. Not. Roy. Astron. Soc.* **497**, 204 (2020), arXiv:2007.00828 [astro-ph.CO].
- [51] O. A. Hannuksela, T. E. Collett, M. Çalışkan, and T. G. F. Li, *Mon. Not. Roy. Astron. Soc.* (2020), 10.1093/mnras/staa2577, arXiv:2004.13811 [astro-ph.HE].
- [52] O. A. Hannuksela, K. Haris, K. K. Y. Ng, S. Kumar, A. K. Mehta, D. Keitel, T. G. F. Li, and P. Ajith, *Astrophys. J.* **874**, L2 (2019), arXiv:1901.02674 [gr-qc].
- [53] E. L. Turner, J. P. Ostriker, and J. R. Gott, III, *Astrophys. J.* **284**, 1 (1984); O. Moeller, M. Kitzbichler, and P. Natarajan, *Mon. Not. Roy. Astron. Soc.* **379**, 1195 (2007), arXiv:astro-ph/0607032 [astro-ph].
- [54] S. Weinberg, *Cosmology* (Oxford, UK: Oxford Univ. Pr. (2008) 593 p, 2008).
- [55] Y.-Y. Choi, C. Park, and M. S. Vogeley, *Astrophys. J.* **658**, 884 (2007), arXiv:astro-ph/0611607 [astro-ph].
- [56] K. Yagi and N. Seto, *Phys. Rev. D* **83**, 044011 (2011), [Erratum: *Phys. Rev. D* 95, 109901 (2017)], arXiv:1101.3940 [astro-ph.CO].
- [57] T. Nakamura *et al.*, *PTEP* **2016**, 093E01 (2016), arXiv:1607.00897 [astro-ph.HE]; S. Isoyama, H. Nakano, and T. Nakamura, *PTEP* **2018**, 073E01 (2018), arXiv:1802.06977 [gr-qc].
- [58] A. Nitz *et al.*, “gwastro/pycbc: Pycbc release v1.13.6,” (2019).
- [59] S. Mirshekari, N. Yunes, and C. M. Will, *Phys. Rev. D* **85**, 024041 (2012), arXiv:1110.2720 [gr-qc].
- [60] M. Dominik, K. Belczynski, C. Fryer, D. E. Holz, E. Berti, T. Bulik, I. Mandel, and R. O’Shaughnessy, *Astrophys. J.* **779**, 72 (2013), arXiv:1308.1546 [astro-ph.HE].
- [61] M. Dominik, K. Belczynski, C. Fryer, D. Holz, E. Berti, T. Bulik, I. Mandel, and R. O’Shaughnessy, *Astrophys. J.* **759**, 52 (2012), arXiv:1202.4901 [astro-ph.HE].
- [62] S. R. Taylor and J. R. Gair, *Phys. Rev. D* **86**, 023502 (2012), arXiv:1204.6739 [astro-ph.CO].
- [63] E. Poisson and C. M. Will, *Gravity: Newtonian, Post-Newtonian, Relativistic* (Cambridge University Press, 2014).
- [64] L. S. Finn, *Phys. Rev. D* **53**, 2878 (1996), arXiv:gr-qc/9601048.